Neuroscience 247 (2013) 12–24

THE NEUROKININ-3 RECEPTOR (NK_3R) ANTAGONIST SB222200 PREVENTS THE APOMORPHINE-EVOKED SURFACE BUT NOT NUCLEAR NK_3R REDISTRIBUTION IN DOPAMINERGIC NEURONS OF THE RAT VENTRAL TEGMENTAL AREA

S. HETHER, K. MISONO AND A. LESSARD *

Maryland Psychiatric Research Center, University of Maryland School of Medicine, Baltimore, MD 21228, United States

Abstract—Schizophrenia is a severe condition that has been associated with functional abnormalities in dopaminergic (DA) neurons of the ventral tegmental area (VTA). Neurokinin-3 receptors (NK_3Rs) of the tachykinin family of neuropeptides modulate the activity of VTA DA neurons and might be involved in DA abnormalities relevant to schizophrenia. Recent work from our lab showed that systemic injection of the dopamine D1/D2 receptor agonist apomorphine in rats, which mimics schizophrenia-like behaviors in humans, also evoked a redistribution of NK_3Rs in DA neurons of the rat VTA. In the present study, VTA microinjection of the selective NK_3R antagonist SB222200 (1 nmol/0.2 μl) or the nuclear import blocker SN50 (2 μg/0.2 μl) was performed in awake rats 10 min prior to systemic injection of apomorphine. VTA sections were dual immunolabeled for the NK_3R (immunogold) and the dopamine synthesizing enzyme tyrosine hydroxylase (TH, immunoperoxidase). Electron microscopic quantifications of somatic and dendritic densities of NK_3 immunogold particles were compared in rats receiving central and systemic injections. In DA (TH-labeled) dendrites, VTA microinjection of SB222200 prevented the apomorphine-evoked decrease in surface NK_3R density as well as the apomorphine-induced increase in cytoplasmic NK_3R density. In contrast, VTA microinjection of SN50, but not SB222200, prevented the apomorphine-induced increase in nuclear NK_3R density. VTA microinjection of SB222200 or SN50 without apomorphine had no effect on the NK_3R distribution or density in TH and non-TH profiles within the VTA. In non-TH, presumably GABAergic neurons of the VTA, the NK_3R densities in somata and dendrites were not significantly changed by apomorphine with or without SB222200. The results suggest that the NK_3R antagonist SB222200 is effective against the apomorphine-evoked NK_3R internalization in VTA DA dendrites, but does not prevent nuclear NK_3R trafficking in VTA DA neurons. These results might have important implications in targeting NK_3R antagonists in basic or clinical studies. Published by Elsevier Ltd. on behalf of IBRO.

Key words: peptide receptors, tachykinin, mesocorticolimbic circuitry, dopaminergic neurons, substance P, schizophrenia.

INTRODUCTION

The neurokinin-3 receptor (NK_3R) of the tachykinin family of neuropeptides belongs to the group of heptahelical transmembrane G protein-coupled receptors (GPCRs), a group of cell surface mediators that activate a cascade of enzymatic signaling pathways leading to acute (cell activation) or delayed (genomic) cellular responses. NK_3 receptors (NK_3Rs) activate neurons by releasing intracellular calcium through the phospholipase C/inositol triphosphate signaling pathway (Regoli and Boudon, 1994). In addition to this primary cellular effect, NK_3Rs might carry out an additional function at the cell nucleus. Indeed, NK_3Rs belong to a novel sub-group of nuclear GPCRs representing receptors that have been identified in the cell nucleus; these include the NK_3R but not the neurokinin-1 or neurokinin-2 receptors (Lee et al., 2004; Jensen and Zhang, 2008; Lessard et al., 2009). The NK_3R and other nuclear GPCRs share a putative nuclear localization signal motif (NLS) sequence that is mainly located in their C-terminal portion (Lee et al., 2004). The NLS sequence is suggested to contribute to nuclear importation of these GPCRs by specific binding with chaperone proteins such as importins (Chahine and Pierce, 2009; Jensen and Sundstrom, 2010). Although their function is unknown, the presence of nuclear NK_3Rs suggests that they might be involved in gene transcription.

We observed nuclear NK_3Rs in dopaminergic (DA) and non-DA mesocorticolimbic projection neurons of the rat ventral tegmental area (VTA) as well as in human NK_3R transfected cells (Lessard et al., 2007, 2009). Activation of VTA NK_3Rs increases dopamine release locally as well as in VTA projection neurons targeting the nucleus accumbens (Acb) and the medial prefrontal

*Corresponding author. Address: Department of Psychiatry, Maryland Psychiatric Research Center, University of Maryland School of Medicine, Maple and Locust Streets, Baltimore, MD 21228, United States. Tel: +1-410-402-6813; fax: +1-410-402-6066.

E-mail address: alessard@mprc.umaryland.edu (A. Lessard).

Abbreviations: Acb, nucleus accumbens; ANOVA, analysis of variance; BDMA, benzyldimethylamine; DA, dopaminergic; DDSA, dimethyl sulfoxide; DMSO, dodecenyl succinic anhydride; DPX, dibutyl phthalate xylene; EMbed 812, epichlorohydrin epoxin resin for embedding; GPCRs, G protein-coupled receptors; mPFC, medial prefrontal cortex; NMA, nadic(R),methyl anhydride; NF-κB, nuclear factor kappa-B; $NK_{1,2,3}$, neurokinin-1,2,3; NK_3R, neurokinin-3 receptor; NK_3Rs, neurokinin-3 receptors; NKA, neurokinin A; NKB, neurokinin B; NLS, nuclear localization signal motif; PB, phosphate buffer; SHR, spontaneously hypertensive rat; SNc, substantia nigra *pars compacta*; SNr, substantia nigra *pars reticulata*; SP, substance P; TH, tyrosine hydroxylase; VTA, ventral tegmental area.

0306-4522/13 $36.00 Published by Elsevier Ltd. on behalf of IBRO.
http://dx.doi.org/10.1016/j.neuroscience.2013.05.006

cortex (mPFC) (Stoessl et al., 1991; Tremblay et al., 1992; Humpel and Saria, 1993; Seabrook and Bowery, 1995; Nalivaiko et al., 1997; Marco et al., 1998). The potential role of nuclear NK_3Rs in the modulation of these DA neurons, however, is unknown.

We recently reported that systemic injection of the DA D_1/D_2 receptor agonist apomorphine evokes a redistribution of NK_3Rs in DA neurons of the VTA, without affecting the NK_3R localization in non-DA, presumably GABAergic VTA neurons (Misono and Lessard, 2012). The redistribution might reflect dendritic internalization of the NK_3R (decrease in plasmalemmal accompanied by an increase in cytoplasmic densities) and nuclear NK_3R translocation. In the present study, unilateral VTA microinjection of the selective NK_3R antagonist SB222200 or the nuclear import blocker SN50 was performed in awake rats 10 min before systemic apomorphine injection. Quantitative electron microscopic evaluation of dendritic and somatic NK_3R densities revealed that (1) VTA microinjection of SB222200 prevented the apomorphine-evoked changes in dendritic NK_3R densities, but not the apomorphine-evoked increase in nuclear NK_3R density while (2) VTA microinjection of SN50 blocked the apomorphine-evoked increase in nuclear NK_3R density in DA neurons within the VTA.

The involvement of NK_3Rs in normal and abnormal DA neurophysiology is poorly understood. Although NK_3R antagonists showed promising results in clinical trials (Meltzer et al., 2004), subsequent reports have been disappointing by showing no improvement on positive or negative symptoms in schizophrenics (Griebel, 2012a). Our results reveal that the selective NK_3R antagonist SB222200, while effective in preventing an apomorphine-evoked NK_3R internalization in dendrites, cannot prevent its translocation to the nucleus. It is conceivable that NK_3R antagonists failed in clinical trials partly because they cannot prevent the activity of nuclear NK_3Rs that might be involved in the pathology of schizophrenia.

EXPERIMENTAL PROCEDURES

Animals

Male Sprague–Dawley rats (280–350 g) were purchased 14 days prior to their experimental use (Charles River Laboratories, Kingston, NY, USA). All animals (n = 24) were housed two per cage in a colony room under a 12-h light/dark cycle. Food and water were available *ad libitum.* Each rat was used for only one experiment. All experiments were conducted in accordance with the National Institute of Health (NIH) regulations of animal care and were approved by the Institutional Animal Care and Use Committee of the University of Maryland School of Medicine.

Guide cannulae implantation and drug administration in awake rats

Rats were anesthetized with a mixture of ketamine–xylazine (100 and 10 mg/kg, respectively, i.p., Fort Dodge, IA, USA), then positioned on the stereotaxic frame (Stoelting, Wood Dale, IL, USA) with the incisor set at 3.3 mm below the interaural line. The skull was exposed, cleaned and a hole was drilled 5.3 mm posterior to Bregma (Paxinos and Watson, 2007). A 23-gauge stainless steel guide cannula was targeted 2 mm dorsal to the VTA, and implanted at 0.7 mm lateral to the midline and 6.5 mm ventral to the skull surface, fixed with two screws and dental cement. A stylet (31-gauge stainless steel, Small Parts, Logansport, IN, USA) was inserted into the guide cannula to prevent cerebrospinal fluid occlusion. Rats received rimadyl (5 mg/kg, s.c. before the surgery as well as 24 and 48 h post-surgery) and lidocaine ointment (Butler Schein, Dublin, OH, USA), then allowed to recover for 7 days.

All rats were handled for 10 min daily starting 1 week before the experiment to minimize stress by manipulation. On the day of the experiment, animals were moved to a quiet testing room at least 30 min prior to drug treatment. Each rat received a single VTA microinjection of SB222200 or SN50 (or their respective vehicle) and a single s.c. injection of apomorphine or vehicle. A 31-gauge stainless steel injector was then inserted in the VTA guide cannula without handling the rats. The injector extended 2 mm beyond the previously implanted guide cannula and was connected to a Hamilton 5 μl microsyringe (Fisher Scientific) via a PE-10 polyethylene tubing (Intramedics, Clay Adams, Parsippany, NJ, USA). SB222200 (1 nmol/0.2 μl; Tocris, Bristol, UK), SN50 (2 μg/0.2 μl; EMD Millipore, Billerica, MA, USA) or their vehicle solution was microinjected in awake rats over a period of 1 min. Dose and injection volume of SB222200 and SN50 are based on previous *in vivo* studies demonstrating efficacy when microinjected in rats (Kelly et al., 2003; Lessard et al., 2004; Deschamps and Couture, 2005; De Brito Gariepy and Couture, 2010). Vehicle solutions were artificial cerebrospinal fluid (Harvard Bioscience, Holliston, MA, USA) for SN50 and artificial cerebrospinal fluid containing 13% or less of Dimethyl Sulfoxide (DMSO) (Sigma) for SB222200. Ten minutes after VTA microinjection, 1 mg/kg apomorphine (R-(−)-Apomorphine-HCl, Sigma) or its vehicle (isotonic saline containing 0.1 mg/ml ascorbic acid) was injected subcutaneously (s.c.). The animals were anesthetized 60 min after the systemic injection for perfusion-fixation of their brain tissue. This time-course is based on several studies showing trafficking of neurokinin-1 and NK_3Rs as well as changes in SP content in the rodent midbrain 60 min after systemic injection of apomorphine (Shirayama et al., 2000; Lessard and Pickel, 2005; Misono and Lessard, 2012).

Antisera

NK_3R localization was achieved by using a rabbit polyclonal antiserum raised against a C-terminus peptide sequence of the rat NK_3R (Novus Biologicals®, Littletown, CO, USA). This antiserum showed high levels of specificity when tested by techniques of preadsorption, transfection and radioimmunoassay, where it produced a single band around 70 kDa by

Western blot (Grady et al., 1996; Seybold et al., 1997; Oyamada et al., 1999; Lessard et al., 2009). This antiserum also shows minimal non-specific immunolabeling of 0.5% or less in compartments not known to express NK_3Rs (e.g. myelin), no cross-reaction of secondary immunomarkers, a similar profile labeling using immunogold and immunoperoxidase, and a significant difference between the actual quantitative distribution of the receptor, and the calculated random distribution, suggesting a non-random distribution of NK_3Rs in the rat VTA (Lessard et al., 2009). In resting conditions, NK_3R immunolabeling shows regional differences, where nuclear labeling is absent (hypothalamus) or abundant (VTA) in sections processed with NK_3R antisera targeting N- or C-terminal portions of the receptor (Jensen and Zhang, 2008; Sladek et al., 2011; Misono and Lessard, 2012). The DA phenotype was distinguished by using a mouse monoclonal antibody raised against the enzyme tyrosine hydroxylase (TH), which was commercially obtained from Incstar (Stillwater, MN, USA). The antiserum exclusively recognizes TH, and no other catecholamine-synthesizing enzymes (Pickel et al., 1975). Thus, both antisera used in this study are well characterized and shown to have high specificities for their respective antigens.

Tissue preparation and electron microscopic single and dual immunolabeling

Sixty minutes after the acute injection of apomorphine or vehicle, rats were deeply anesthetized by an i.p. injection of 500–600 mg/kg chloral hydrate. The anesthetized animals were perfused through the aortic arch with 5–10 ml of saline, 50 ml of 3.75% acrolein in 2% paraformaldehyde and 200 ml of 2% paraformaldehyde in 0.1 M phosphate buffer (PB), pH 7.4. The brains were removed from the cranium and fixed with 2% paraformaldehyde for 30 min. A rostrocaudal sequence of brain sections (40 μm) was prepared using a Vibratome (Leica Microsystems®, Bannockburn, IL, USA). VTA sections of tissue were then placed in 1% sodium borohydride for 30 min to neutralize reactive aldehydes as described in prior studies using acrolein fixation (Leranth and Pickel, 1889).

The prepared sections were processed for dual immunogold silver and peroxidase labeling of antisera before plastic embedding (Chan et al., 1990). This approach was used to enable high-resolution detection of plasma membrane and intracellular distributions of receptors that can be lost during the process of plastic embedding (Adams et al., 2002). To minimize penetration problems inherent to the pre-embedding methodology, the sections were cryoprotected in 25% sucrose and 3.5% glycerol in PB, and then incubated 10 min at −80 °C at decreasing concentrations of the cryoprotectant solution (100%; 70%; 50%; 30% and 0% or 100% PB). The freeze–thaw method produces minute holes in the tissue allowing greater penetration of immunoreagents. Some sections were single immunolabeled for TH to confirm the microinjection site in the VTA; these were not processed for freeze–thaw, however Triton X-100 (0.25%) was added in the primary antiserum solution.

VTA sections for single (light microscopy) and dual (electron microscopy) immunolabeling were incubated for 24 h at room temperature. Sections processed for electron microscopy were incubated at 4 °C for another 12 h in a solution containing mouse anti-TH antisera (peroxidase) with (dual) or without (single) rabbit anti-NK_3R (immunogold) at dilutions of 1:50,000 and 1:1000, respectively. After this incubation, the sections were rinsed and placed for 30 min in biotinylated secondary goat anti-mouse IgG (1:400, Incstar) followed by the ABC complex (ABC; Vector, Burlingame, CA, USA) for detection of the mouse TH antibody. The bound peroxidase was identified by reaction of the sections for 6 min in 3,3′-diaminobenzidine (Aldrich Chemicals, Milwaukee, WI, USA) and hydrogen peroxide. Sections processed for light microscopy were mounted onto gelatin-coated slides, air dried, dehydrated through alcohols and xylenes, and then mounted beneath glass coverslips with dibutyl phthalate xylene (DPX) mounting medium (Aldrich). The slides were examined using a Zeiss light microscope (Jena, Germany), and images were captured using an Olympus DP70 digital camera (Center Valley, PA, USA).

Sections processed for electron microscopy were rinsed in Tris buffer (0.1 M, pH 7.6), and placed for 2 h in a 1:50 dilution of donkey anti-rabbit IgG with bound 1 nm colloidal gold (Amersham, Arlington, IL, USA) for detection of the rabbit NK_3R antiserum. The gold particles were fixed to the tissue by incubation of the sections in 2% glutaraldehyde in 0.01 M phosphate buffered saline for 10 min. The particles were enlarged for microscopic examination by reaction in a silver solution from the IntenS-EM kit (Ted Pella, Redding, CA, USA) for 7 min at room temperature (see Chan et al., 1990). The sections were then postfixed in 2% osmium tetroxide in 0.1 M PB, dehydrated and flat-embedded in epon (19% epichlorohydrin epoxin resin for embedding (EMbed 812); 36% dodecenyl succinic anhydride (DDSA); 44% nadic (R),methyl anhydride (NMA); 1% benzyldimethylamine (BDMA); Electron Microscopy Sciences, Fort Washington, PA, USA) between two pieces of Aclar plastic (Electron Microscopy Sciences, Fort Washington, PA, USA). To minimize between group variations in quantification of NK_3 immunogold particles, VTA sections from vehicle and SB222200 or SN50-treated rats with systemic apomorphine or vehicle-injections were co-processed under identical labeling conditions.

Ultrathin sections from the outer surface of each Vibratome section in the region of the VTA at coordinates 5.0–5.5 mm posterior to the bregma (Paxinos and Watson, 2007) were collected onto grids by using an ultramicrotome (Nova, Bromma, Sweden). The criterion used for a successful VTA microinjection site is the presence of the injector tip within a range of 0.5 mm from the VTA, a distance range where NK_3R agonists and antagonists showed significant cardiovascular and behavioral effects in rats

(Deschamps and Couture, 2005; De Brito Gariepy and Couture, 2010). The sections on grids were counterstained with Reynold's lead citrate and uranyl acetate. The thin sections were examined by using a Hitachi H7000 transmission electron microscope. Images were captured using an AMT digital camera, then imported to Photoshop software (Adobe Systems, Mountain View, CA, USA), and adjusted for sharpness only. The final images were then imported to Power Point software (Microsoft Windows®) for assembly and labeling composite figures.

Data analysis

To assess the distribution of NK_3R immunogold particles, data analysis was performed on ultra-thin sections exclusively obtained from the surface (1–2 μm) of the flat-embedded tissue, where there was optimal penetration of immunoreagents. The profiles containing NK_3 immunoreactivity were classified as either neuronal (dendrites, axon terminals) or glial based on well-established criteria (Peters et al., 1991). Peroxidase immunoreactive profiles had an electron density considerably greater than that seen in comparable structures in the surrounding neuropil that were considered unlabeled. The normal subcellular distribution of NK_3Rs in the rat VTA was previously investigated (Lessard et al., 2007, 2009). Non-specific labeling was assessed by quantification of NK_3 immunogold particle on the myelin, revealing a false-positive labeling of less than 0.5% of identified structures. In addition, we observed a similar distribution when the secondary immunomarkers (immunogold for TH, immunoperoxidase for NK_3R) were reversed (Lessard et al., 2007).

To measure trafficking of NK_3Rs, NK_3-labeled dendrites with or without TH labeling were captured and quantitatively analyzed. To minimize experimental variables that could affect group comparisons, VTA sections of all eight groups of rats: (1) vehicle (VTA)–vehicle (s.c.); (2) SB222200 or SN50 (VTA)–vehicle (s.c.); (3) vehicle (VTA)–apomorphine (s.c.) and (4) SB222200 or SN50 (VTA)–apomorphine (s.c.) were co-processed in the same antisera solutions. Moreover, the data analysis was performed by an investigator that was blind to the conditions. The profile diameter, area and perimeter were measured by using Image J software (National Institute of Health, JAVA 1.60_02). One to four vibratome sections per animal were examined, and each section generated at least 50 images of magnifications ranging from 7000× to 40,000×. A total area of 89,346 μm^2 of the VTA was examined in all experimental groups for the SB222200 project: vehicle–vehicle, 16,171 μm^2; SB222200–vehicle, 12,515 μm^2; vehicle–apomorphine, 18,294.168 μm^2 and SB222200–apomorphine, 16,318.74 μm^2 and the SN50 project: vehicle–vehicle, 3433.66 μm^2; SN50–vehicle, 6359.181 μm^2; vehicle–apomorphine, 5092.08 μm^2 and SN50–apomorphine, 11,162.904 μm^2. Parameters used for statistical comparisons were (1) the number of gold particles in contact with the plasma membrane/perimeter of individual profile, (2) the number of gold particles not in contact with the plasma membrane/profile area, (3) the number of gold particles on the nucleus/nucleus area and (4) the number of gold particles on the somata excluding nucleus/area of somata without the nucleus. Data were also analyzed as percentage (%) of plasmalemmal NK_3 immunogold particles/total number of NK_3 immunogold particles in non-DA and DA dendrites. The plasmalemmal immunolabeling is defined as NK_3 immunogold particles in direct contact with the plasma membrane (no distance allowed between the immunogold particle and the plasma membrane). Results are expressed as means ± S.E. mean of (*n*) rats. Results were analyzed for statistical significance using one-way analysis of variance (ANOVA) followed by a Bonferroni post hoc test (ratios 1–4) or Chi-square (%) using SPSS software (Windows® Lead Technologies). Only probability values (*P*) less than 0.05 were considered to be statistically significant.

RESULTS

Light microscopic evaluation of microinjection sites in the VTA

Microinjection sites were examined by light microscopy in sections showing intense TH-immunolabeling throughout the paranigral and parabrachial portions of the VTA (indicated by the dashed line in Fig. 1). All microinjection sites (n = 24 rats) were within a distance of 0.5 mm or less from the VTA and included in the data analysis (Fig. 1). The vast majority (n = 17 rats) of the microinjection sites were located in the middle rostrocaudal VTA (5.3 mm posterior to Bregma), while others were located slightly anterior (5.0 mm posterior to Bregma, n = 6 rats) or posterior (5.5 mm posterior to Bregma, n = 1 rat) to this area (Paxinos and Watson, 2007). There were no signs of hemorrhage, atrophy, sclerosis, thrombosis or any other type of neuronal abnormality.

NK_3R distribution and density in VTA DA and non-DA profiles following of VTA microinjection of SB222200

Quantitative or qualitative differences were not found between vehicle–vehicle and SB222200–vehicle-treated rats in the distribution of NK_3 immunogold particles in different DA or non-DA neuronal compartments (soma, dendrites, and axon terminals), as well as their plasmalemmal, cytoplasmic and nuclear NK_3R densities (ANOVA one-way followed by Bonferroni post hoc test; data not shown). In addition, the distribution and density of NK_3Rs in both groups were also similar to those reported in our previous studies using rats under control conditions (Lessard et al., 2007, 2009; Misono and Lessard, 2012). Since SB222200 had no effect on NK_3R distribution and density, rats from vehicle-vehicle and SB222200–vehicle groups were pooled together as the control group for the quantitative measurements of NK_3 immunogold particles in VTA profiles of rats receiving apomorphine with or without prior VTA microinjection of SB222200.

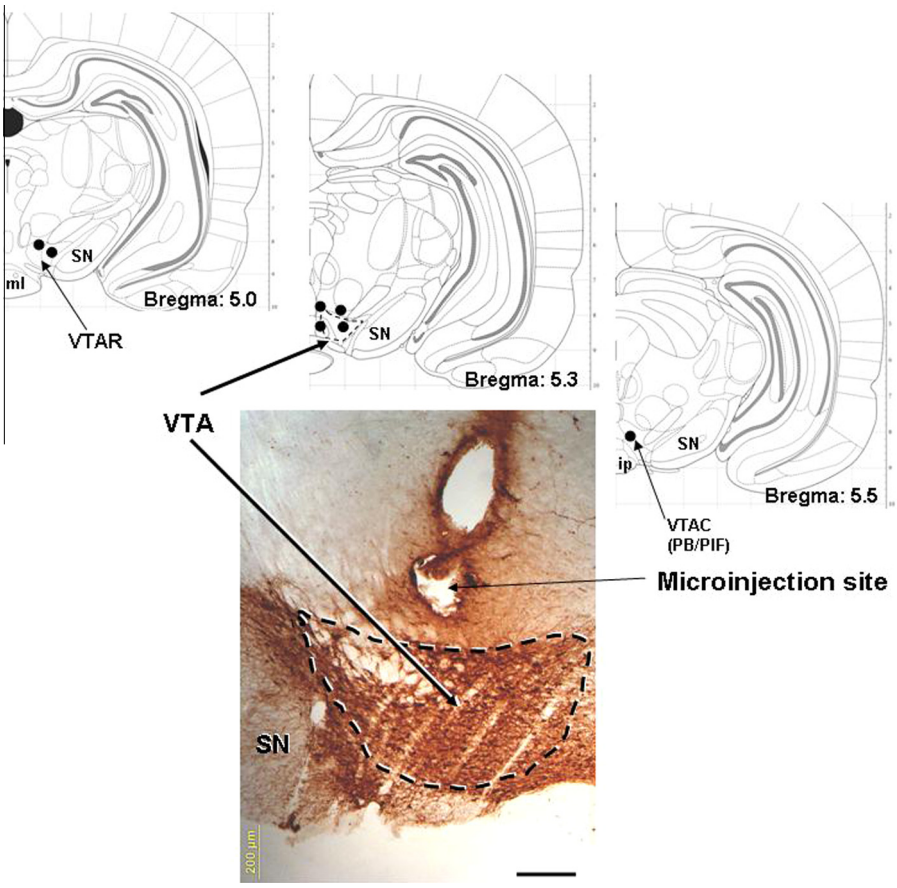

Fig. 1. Identification of microinjection sites in the paranigral and parabrachial portions of the ventral tegmental area (VTA; showed by the dashed line) immunolabeled for tyrosine hydroxylase. Modified pictures from an atlas (Paxinos and Watson, 2007) and light microscopic picture showing the position of the injector tips (black circles). The vast majority (n = 17 rats) of microinjection sites were located in the medial VTA (5.3 mm posterior to Bregma), while few were observed slightly anterior (5.0 mm posterior to Bregma, n = 6 rats) or posterior (5.5 mm posterior to Bregma, n = 1 rat) to the medial VTA. ip, interpeduncular nucleus; ml, medial mammilary nucleus; PB, parabrachial pigmented nucleus of the VTA; PIF, parainterfascicular nucleus of the VTA; SN, substantia nigra; VTAR, rostral portion of the VTA; VTAC, caudal portion of the VTA. Scale bar = 200 µm.

VTA microinjection of SB222200 on the apomorphine-evoked trafficking of NK_3Rs in VTA DA and non-DA dendrites

Consistent with our previous study (Misono and Lessard, 2012), systemic apomorphine decreased NK_3R densities on plasmalemmal portion of DA dendrites and increased NK_3R densities on cytoplasmic portions of DA dendrites. In contrast, apomorphine did not alter the NK_3R distribution or densities in non-DA dendrites (Fig. 2). VTA microinjection of SB222200 prevented the apomorphine-evoked changes in NK_3R densities in DA dendrites (Fig. 2). A quantitative analysis of NK_3R densities was performed in transversely cut dendrites of a comparable size (cross-sectional diameter range of 0.5–2 µm). Ratios of the number of NK_3 immunogold particles in contact with the plasma membrane/perimeter of dendrite and the number of NK_3 immunogold particles in the cytoplasm/area of dendrite were compiled in individual dendrites with or without TH immunoreactivity. As compared to TH-immunolabeled dendrites from the control group that includes rats receiving systemic vehicle solution with or without VTA microinjection of SB222200, TH dendrites from the apomorphine-injected rats contained significantly fewer NK_3 immunogold particles on the plasma membrane (Fig. 3). The apomorphine-induced decrease in plasmalemmal NK_3R density was prevented in animals that received VTA microinjection of SB222200 (Fig. 3). The same result was obtained using the percent of NK_3 plasmalemmal immunolabeling in TH-labeled dendrites from control, apomorphine and SB222200–apomorphine groups of rats (Table 1). In non-DA dendrites, no significant changes were observed in the percent of plasmalemmal proportion of NK_3Rs between apomorphine- and vehicle-treated animals in the presence or absence of VTA injection of SB222200 (data not shown).

Consistent with earlier results, TH-labeled dendrites from rats receiving apomorphine without SB222200 contained a higher density of NK_3 immunogold particles in the cytoplasm as compared to the control group (Fig. 3). VTA microinjection of SB222200 significantly prevented the apomorphine-evoked increase in the number of NK_3 immunogold particles in the cytoplasm

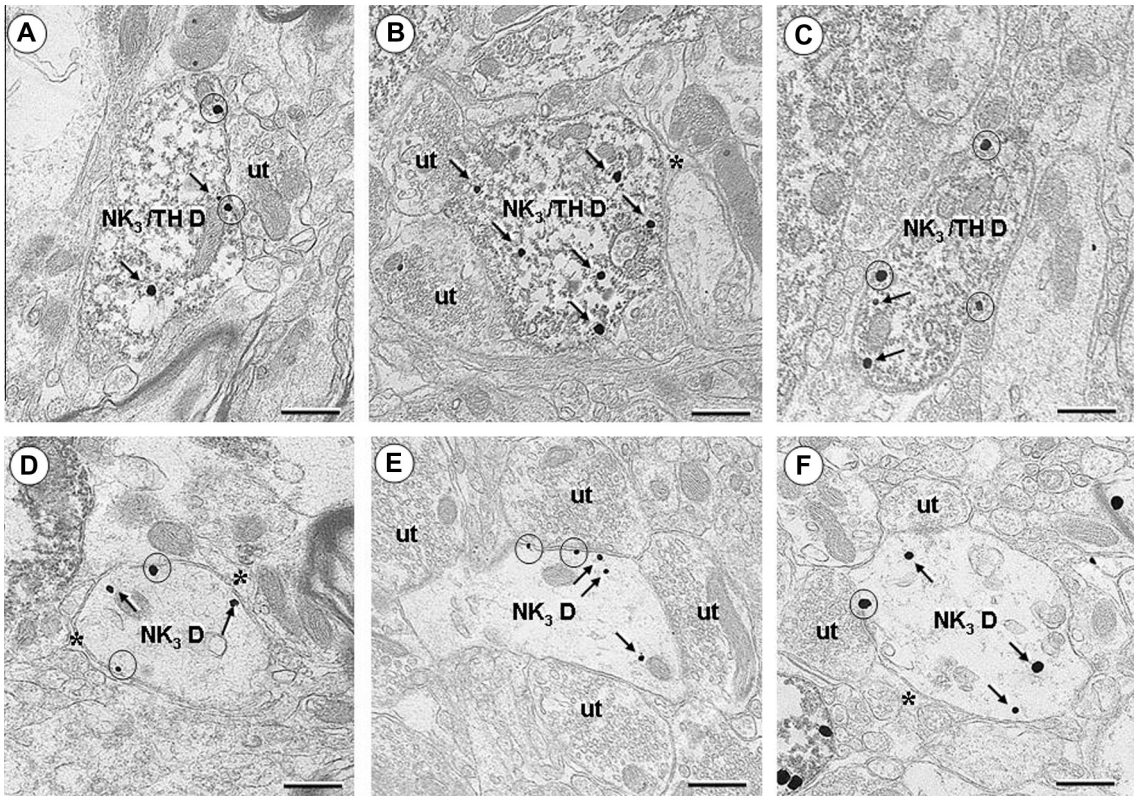

Fig. 2. Electron micrographs showing plasmalemmal (encircled) and cytoplasmic (arrows) distribution of NK_3R immunogold particles in VTA dopaminergic (NK_3/TH D; A–C) and non-dopaminergic (NK_3 D; D–F) dendrites of rats receiving VTA microinjection of SB222200 and systemic vehicle (A, D), VTA microinjection of the vehicle solution and systemic apomorphine (B, E) and VTA microinjection of SB222200 and systemic apomorphine (C, F). Cross-sectional dendrites are surrounded by astrocyte processes (asterisk) or unlabeled terminals (ut). In dopaminergic dendrites, the apomorphine-evoked changes (plasmalemmal decrease and cytoplasmic increase) in NK_3R densities (B) appear to be reversed by prior VTA microinjection of the NK_3R antagonist SB222200 (C). The distribution and density of NK_3 immunogold particles is similar in non-dopaminergic dendrites of rats receiving apomorphine with or without prior VTA microinjection of SB222200 (D–F). Scale bars = 0.5 μm.

(Fig. 3). In non-TH dendrites, apomorphine, with or without VTA microinjection of SB222200, did not alter the distribution or density of NK_3Rs on the plasma membrane or cytoplasmic portions of dendrites (Fig. 3).

VTA microinjection of SB222200 or SN50 on the apomorphine-evoked trafficking of NK_3Rs in VTA DA and non-DA somata and neuronal nuclei

Numerous NK_3 immunogold particles were seen in cytoplasmic as well as nuclear portions of TH and non-TH cell bodies. The vast majority of NK_3 immunogold particles were in the proximity of organelles such as endomembranes resembling smooth endoplasmic reticulum, the rough endoplasmic reticulum, the Golgi apparatus and the mitochondria. Within the nucleus, NK_3 immunogold particles were typically found some distance away from the nuclear membrane and the nucleolus, sometimes clustered together or near suspended perichromatin particles. Apomorphine with or without VTA microinjection of SB222200 did not affect the proportion of NK_3 immunogold particles associated with these endomembranes or the nucleus membrane (data not shown).

There was a qualitative (Fig. 4) and quantitative (Fig. 6) increase in NK_3R density in TH-labeled cytoplasmic and nuclear portions of the soma in apomorphine-treated rats compared to the control group. These results are consistent with our previous study (Misono and Lessard, 2012). Surprisingly, however, prior VTA microinjection of SB222200 failed to prevent the apomorphine-increase in NK_3R cytoplasmic or nuclear density (Fig. 6). The apomorphine-evoked increase in nuclear NK_3R density in DA soma, however, was significantly reduced in animals receiving VTA microinjection of the nuclear import blocker SN50 (Fig. 7). As expected, the NK_3R densities in cytoplasmic and nuclear portions of non-TH somata were not significantly different in vehicle- and apomorphine-treated rats with or without prior VTA microinjection of SB222200 (Figs. 5 and 6).

DISCUSSION

VTA microinjection of the selective antagonist at the NK_3R, SB222200, prevented the apomorphine-evoked redistribution of NK_3Rs in VTA DA dendrites but did not prevent their nuclear translocation. Indeed, the decrease in plasmalemmal as well as the increase in cytoplasmic NK_3R density in DA dendrites in the presence of apomorphine was no longer significant in animals receiving prior VTA microinjection of SB222200.

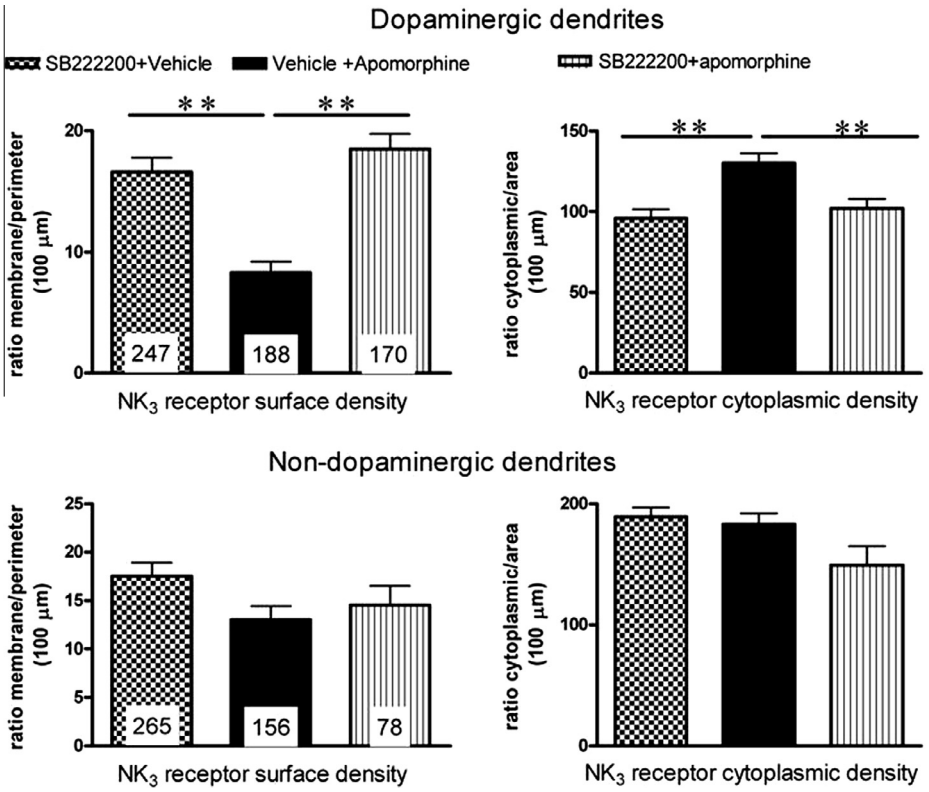

Fig. 3. Bar graphs showing the plasmalemmal (surface) and cytoplasmic density of NK_3 immunogold particles in VTA dopaminergic and non-dopaminergic dendrites of rats receiving VTA microinjection of SB222200 or its vehicle with systemic injection of apomorphine or its vehicle. Data were obtained from at least four vibratome sections per group, each of which covered a minimal area of 1000 μm^2. Vertical bars represent the mean ± S.E. mean in the ratio of the gold particles in contact with the plasma membrane/perimeter of dendrites and number of gold particles in the cytoplasm/area of the dendritic profile (100 μm^2) in dopaminergic and non-dopaminergic dendrites. Numbers in bars represent the number of dendrites measured in each category. The control group represents animals receiving VTA injection of SB222200 or its vehicle and systemic vehicle injection. Statistical comparisons were made between control rats (vehicle–vehicle, $N = 3$ rats and SB222200–vehicle, $N = 3$ rats), VTA microinjection of vehicle and systemic apomorphine- ($N = 3$ rats) and VTA microinjection of SB222200 and systemic apomorphine ($N = 3$ rats). Significant differences were determined using ANOVA one-way followed by a Bonferroni post hoc test. $^{**}P < 0.01$.

Nevertheless, the increase in nuclear NK_3R density in DA somata was not altered in rats receiving VTA microinjection of SB222200. In contrast, VTA microinjection of the nuclear import blocker SN50 prevented the apomorphine-evoked increase in nuclear NK_3R density in DA somata. The evidence suggests that activation of DA receptors could induce internalization of NK_3Rs in DA VTA dendrites and nuclear importation of NK_3Rs in DA VTA somata through two different mechanisms. The apomorphine-induced NK_3R redistribution might reflect (1) activation of pre-synaptic D_1/D_2 DA receptors in striatal axon terminals expressing the endogenous tachykinins SP and NKA (Tamiya et al., 1990; Lu and Ghasemzadeh, 1998; Pickel et al., 2002) and (2) activation of D_2 autoreceptors (Pickel et al., 2002) that would be involved in the nuclear translocation of cytoplasmic NK_3Rs. The results reveal a nontraditional-type of NK_3R trafficking by DA receptor activation, where cytoplasmic NK_3Rs would be translocated in the neuronal nuclei through a signaling pathway not involving internalization of surface NK_3Rs. A summary of the results is presented schematically in Fig. 8.

Table 1. Plasmalemmal NK_3 immunogold distribution (%) in TH-labeled (DA) VTA dendrites in rats receiving VTA microinjection of SB222200 with or without s.c. injection of apomorphine

Treatment	% Plasmalemmal
SB222200 + vehicle (three rats)	34.4 ± 3 ($n = 143$ dendrites)
Vehicle + apomorphine (three rats)	15 ± 2.1 ($n = 200$ dendrites)*
SB222200 + apomorphine (three rats)	35.9 ± 2.3 ($n = 175$ dendrites)

Mean number of gold particles in contact with the plasma membrane/total NK_3 gold particles in VTA TH dendrites. Rats receiving VTA and systemic administration of vehicle solutions had values comparable to the group of rat receiving SB222200 and systemic vehicle solution (36.9 ± 3.4%; $n = 123$ dendrites; $N = 3$ rats).

Chi-square test in between SB222200 + vehicle or SB222200 + apomorphine and vehicle + apomorphine-treated animals.

* $P < 0.01$.

Tachykinin and DA receptor interactions in the rat VTA

As expected, VTA SB222200 injection in resting conditions did not significantly alter the distribution and density of NK_3Rs in the rat VTA. This is consistent with

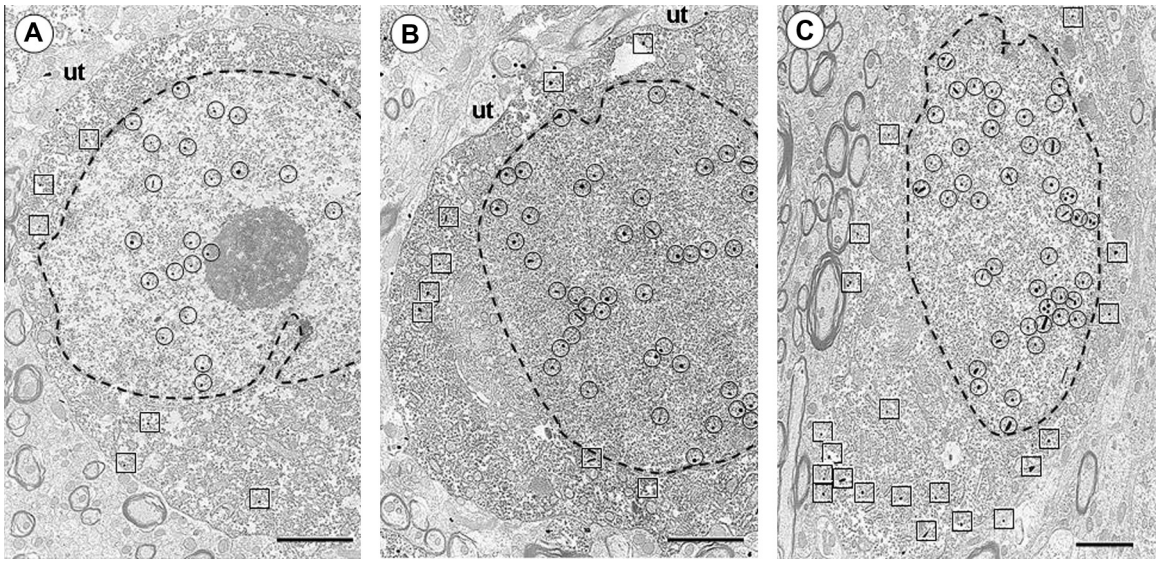

Fig. 4. Electron micrographs of three somata showing immunoperoxidase labeling for TH and many NK_3 immunogold particles located inside (black circles) or outside (black squares) the nuclei in rats receiving VTA microinjection of SB222200 and systemic vehicle (A), VTA microinjection of the vehicle solution and systemic apomorphine (B) and VTA microinjection of SB222200 and systemic apomorphine (C). A soma from apomorphine-treated rats (B) showed an apparent increase in the number of NK_3 immunogold particles inside (black circles) and outside (black squares) the neuronal nuclei, as compared to vehicle-treated rats (A). The apomorphine-evoked increase in nuclear and cytoplasmic NK_3R density appears similar in rats receiving prior VTA microinjection of SB222200 (C). All soma receive inputs from unlabeled terminals (ut). Dashed lines are outlining the nuclear membrane. Scale bars = 2.0 μm.

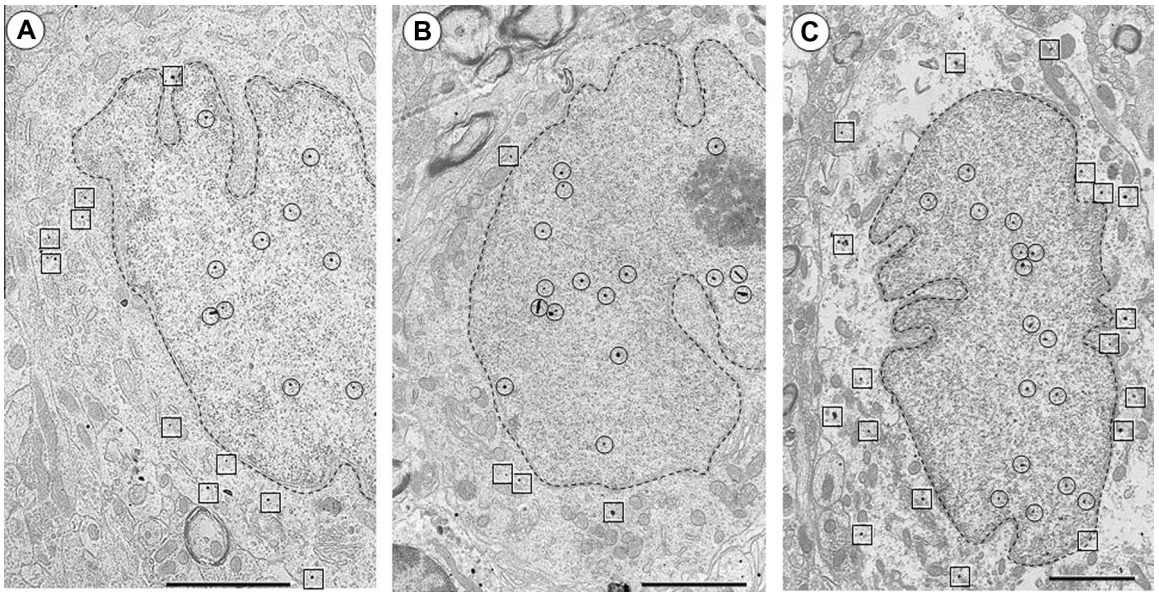

Fig. 5. Electron micrographs of three somata devoid of immunoperoxidase reaction product for TH, and showing NK_3 immunogold particles located inside (black circles) or outside (black squares) the nuclei in rats receiving VTA microinjection of SB222200 and systemic vehicle (A), VTA microinjection of the vehicle solution and systemic apomorphine (B) and VTA microinjection of SB222200 and systemic apomorphine (C). Apomorphine with or without prior VTA microinjection of SB222200 evoked no qualitative change in NK_3R distribution or density in non-TH profiles of the VTA. Dashed lines are outlining the nuclear membrane. Scale bars = 2.0 μm.

the generally accepted concept that tachykinins are mildly activated in normal conditions, yet abundantly released during stress or pathological events such as inflammation, pain and transmitter-related dysfunctional activities (Otsuka and Yoshioka, 1993). Accordingly, several *in vivo* studies showed that microinjection of selective antagonists at the NK_3R in the lateral cerebral ventricle or midbrain areas including the VTA in awake rats had no effect on cardiovascular or behavioral function in resting conditions (Cellier et al., 1997; Lessard et al., 2004; Deschamps and Couture, 2005; De Brito Gariepy and Couture, 2010).

The interaction between neurokinins and dopamine in VTA neurons have been investigated *in vivo* and *in vitro*.

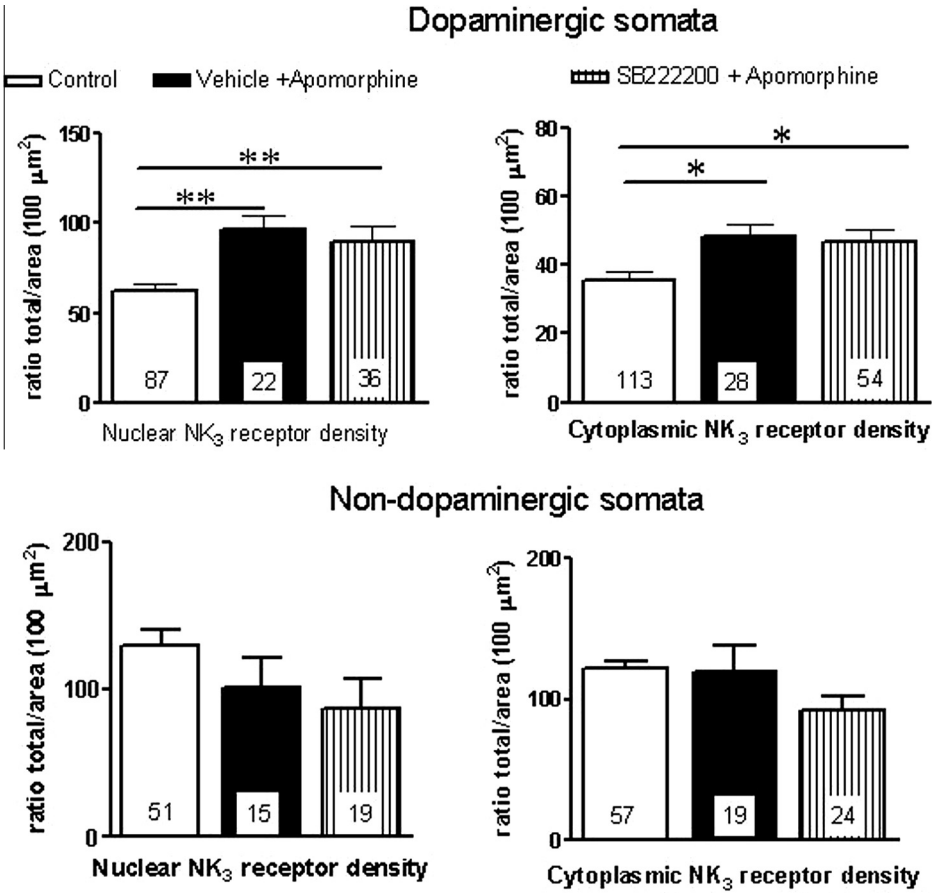

Fig. 6. Bar graphs showing the density of NK_3 immunogold particles in VTA dopaminergic and non-dopaminergic somata of rats receiving VTA microinjection of SB222200 or its vehicle with systemic injection of apomorphine or its vehicle. Data were obtained from at least four vibratome sections per group, each of which covered a minimal area of 1000 μm^2. Vertical bars represent the mean ± S.E. mean in the ratio of the total number of gold particles/area of the profile (100 μm^2) in dopaminergic and non-dopaminergic nuclear or cytoplasmic areas. Numbers in bars represent the number of profiles measured in each category. The control group represents animals receiving VTA injection of SB222200 or its vehicle and systemic vehicle injection. Statistical comparisons were made between control rats (vehicle–vehicle, $N = 3$ rats and SB222200–vehicle, $N = 3$ rats), VTA microinjection of vehicle and systemic apomorphine- ($N = 3$ rats) and VTA microinjection of SB222200 and systemic apomorphine ($N = 3$ rats). Significant differences were determined using ANOVA one-way followed by a Bonferroni post hoc test. $^{*}P < 0.05$; $^{**}P < 0.01$.

In vitro, NK_3R activation promotes dopamine release from VTA projection neurons (Overton et al., 1992; Chen et al., 1998). *In vivo*, cardiovascular and behavioral effects were observed in awake rats receiving VTA microinjections of the selective NK_3R agonist senktide (Deschamps and Couture, 2005; De Brito Gariepy and Couture, 2010). In normal rats, VTA microinjection of senktide evokes rapid (within minutes) increases in heart rate and mean arterial pressure that are accompanied by wet dog shakes, rearing, head scratching, face washing and sniffing behaviors (Deschamps and Couture, 2005). Both cardiovascular and behavioral effects are blocked by prior injection of a NK_3R antagonist (SB235375) or a D_1 receptor antagonist (SHC23390), while treatment with the D_2 receptor antagonist raclopride has no significant effect (Deschamps and Couture, 2005). In contrast, the long-term (8–12 h) anti-hypertensive effect induced by VTA microinjection of NK_3R antagonists (SB222200; R-820) in spontaneously hypertensive rats (SHR) is blocked by the D_2 receptor antagonist raclopride, but only reduced by the D_1 receptor antagonist SCH23390 (De Brito Gariepy and Couture, 2010). Therefore, a tonic activation of VTA NK_3Rs might contribute to high blood pressure in SHR by a mechanism involving the activation of D_2 receptors in mesocorticolimbic DA pathway. This is consistent with behavioral studies reporting schizophrenia-like social deficits and disruption of prepulse inhibition to acoustic startle in SHR, both of which showing improvement following a treatment with D_2 receptor antagonists (Calzavara et al., 2011; Levin et al., 2011). Taken together, these results suggest that acute, presumably ligand–receptor binding activation of VTA NK_3Rs in normal condition evokes rapid physiological responses that most likely involve the activation of D_1 receptors. However, the long-term effects (h) of NK_3R antagonists in pathological conditions (SHR) rather seem to involve the tonic release of tachykinins acting on NK_3Rs and D_2 receptors. These dichotomous acute and chronic effects might be due to a differential surface or nuclear

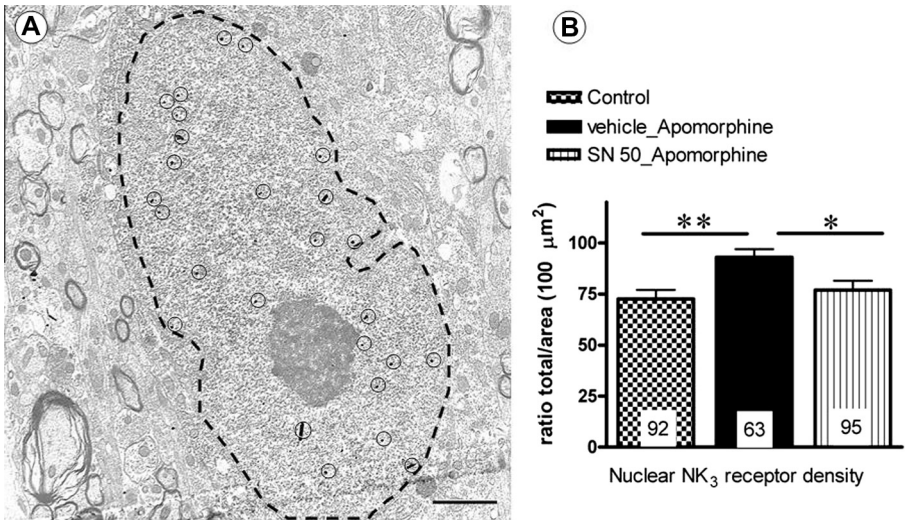

Fig. 7. Electron micrograph (A) and bar graph (B) showing the density of nuclear NK_3 immunogold particles in VTA dopaminergic profiles of animals receiving VTA microinjection of the nuclear import blocker SN50. (A) The number of NK_3 immunogold particles (encircled) located inside the nuclear membrane (dashed line) of VTA DA profiles were calculated in animals receiving SN50 with or without apomorphine injection. Scale bar = 2.0 µm. (B) Ratio of nuclear NK_3R density in control rats, and those receiving systemic apomorphine administrations without or with prior VTA microinjection of SN50. Data were obtained from at least four vibratome sections per group, each of which covered a minimal area of 1000 μm^2. Vertical bars represent the mean ± S.E. mean in the ratio of the total number of gold particles/area of the profile (100 μm^2) in dopaminergic nuclear area. Numbers in bars represent the number of profiles measured in each category. The control group represents animals receiving VTA injection of SN50 or its vehicle and systemic vehicle injection. Statistical comparisons were made between control rats (vehicle–vehicle, $N = 3$ rats and SN50–vehicle, $N = 3$ rats), VTA microinjection of vehicle and systemic apomorphine- ($N = 3$ rats) and VTA microinjection of SN50 and systemic apomorphine ($N = 3$ rats). Significant differences were determined using ANOVA one-way followed by a Bonferroni post hoc test. $^{*}P < 0.05$; $^{**}P < 0.01$.

localization of NK_3Rs and consequent interactions with VTA DA receptors. This possibility deserves further investigations.

Absence of NK_3Rs redistribution following apomorphine in non-TH profiles of the VTA

As previously observed, apomorphine did not alter the NK_3R distribution in non-TH neurons of the VTA (Misono and Lessard, 2012). This heterogenous population of neurons mainly includes GABAergic interneurons and GABAergic projection neurons, but also contains some glutamatergic projection neurons (Carr and Sesack, 2000; Fields et al., 2007; Nair-Roberts et al., 2008). Moreover, a small population of GABAergic neurons in the rat substantia nigra and VTA expresses D_2 receptors (Sesack et al., 1994). These different non-TH phenotypes, which could not be distinguished in our preparation, might also receive differential SP inputs from the striatum or the raphe nucleus (Chan-Palay et al., 1978; Herve et al., 1987; Tamiya et al., 1990; Lu and Ghasemzadeh, 1998). We cannot exclude the possibility that apomorphine evokes significant NK_3R redistribution in one or several of these characterized non-TH phenotypes.

Apomorphine-evoked increase in nuclear NK_3Rs in the rat VTA

Nuclear NK_3Rs have been identified by electron microscopy in the rat VTA and paraventricular nucleus of the hypothalamus (PVN) (Jensen and Zhang, 2008; Lessard et al., 2009; Misono and Lessard, 2012), where nuclear NK_3Rs were co-localized with transciptionally active chromatin in the form of acetylated histones H3 and H4 (Flynn et al., 2011) as well as the carrier protein importin-β (Jensen and Sundstrom, 2010). The mechanism by which GPCRs reach the nucleus remains speculative; however it might be initiated by NLS-dependent contact of the receptor to nuclear import proteins such as importins α- and β that bind with high affinity to proteins of the nuclear pore complex (Pickard et al., 2007; Chahine and Pierce, 2009). In addition, the localization of nuclear NK_3Rs using antisera against the C- and N-terminal portions of the receptor suggests the presence of a full length NK_3R in the neuronal nuclei (Sladek et al., 2011). In the present study, apomorphine-evoked increase in nuclear NK_3Rs in DA somata was not prevented by VTA injection of the selective NK_3R antagonist SB222200. This treatment, however, prevented the apomorphine-evoked redistribution of surface and cytoplasmic NK_3Rs in DA VTA dendrites. The latter result indicates that the dose and injection volume of SB222200 was adequate to prevent internalization of NK_3Rs in the VTA. These results provide evidence to suggest that apomorphine increased the nuclear density of NK_3Rs by a mechanism not involving ligand-binding internalization of surface receptors, but rather through a differential signaling pathway triggered by the activation of a DA receptor. In support of this notion, dopamine D_2 autoreceptors activate the nuclear factor kappa-B (NF-κB) (Yang et al., 2003; Takeuchi and Fukunaga, 2004), a transcription factor endowed with the NLS sequence and imported in the nucleus through the carrier protein importin (Chahine and Pierce, 2009). NK_3Rs in DA

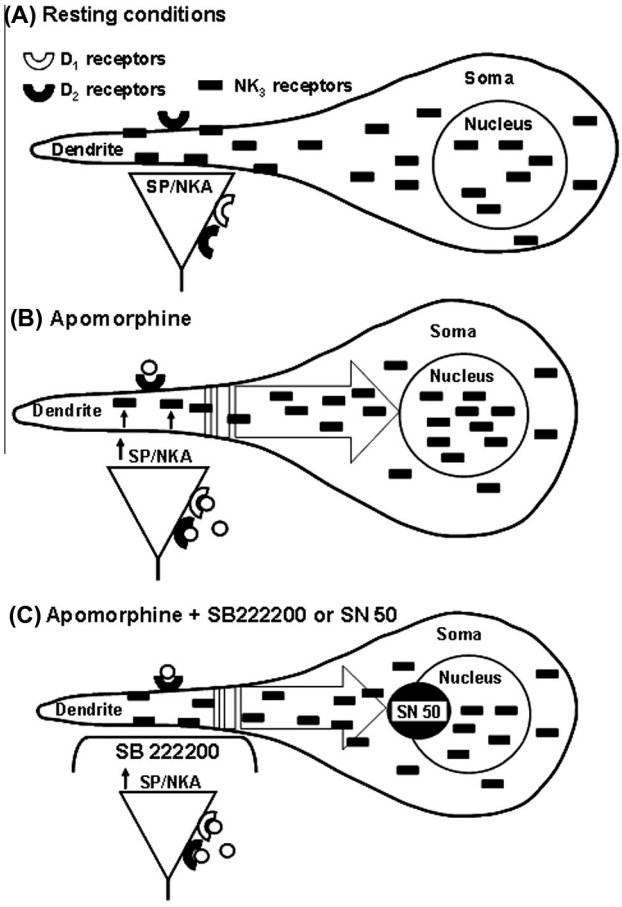

Fig. 8. Differential target areas where SB222200 and SN50 prevent the apomorphine-induced trafficking of NK_3Rs in dopaminergic profiles of the rat VTA. Schematic representation of quantitative electron microscopic (A) distribution of NK_3Rs, dopamine D_1 and D_2 receptors in resting conditions, (B) apomorphine-induced trafficking of the NK_3Rs and (C) effects of VTA microinjections of SB222200 or SN50 on apomorphine-evoked NK_3R redistribution in VTA dopaminergic neurons. The apomorphine-evoked internalization of dendritic NK_3Rs is prevented by the selective NK_3R antagonist SB222200. The apomorphine-induced increase in nuclear NK_3R density, however, is not prevented by SB222200 although the nuclear import blocker SN50 reduced the effect. The apomorphine-evoked nuclear translocation of NK_3Rs might prominently reflect internal trafficking from the cytoplasmic pool, and less likely ligand-binding internalization of plasmalemmal NK_3Rs. These changes in NK_3R densities are not observed in non-TH, presumably GABAergic neurons of the VTA. SP, substance P; NKA, neurokinin A.

neurons of the VTA might then be imported in the neuronal nucleus through a D_2 receptor-mediated signaling pathway along with NF-κB. To test this hypothesis, the nuclear import blocker SN50 was injected in the VTA to confirm a NLS-dependent nuclear importation of NK_3Rs following apomorphine administration. SN50 is a membrane permeable synthetic peptide endowed with the NLS sequence that reduces NF-κB nuclear importation *in vitro* presumably by saturating the importin transporters (Lin et al., 1995). Our results showed that SN50 prevented the apomorphine-evoked increase in nuclear NK_3Rs in DA VTA neurons. This is consistent with prior *in vivo* studies where the central injection of SN50 in anesthetized rats reduced a LPS or DA-induced NF-κB activation (Luo et al., 1999; Kelly et al., 2003). Although our results are in agreement with NLS-dependent NK_3R translocation, we cannot exclude the possibility that an additional nuclear import mechanism is involved in the apomorphine-induced increase in nuclear NK_3R density in VTA DA neurons.

CONCLUSION

NK_3R antagonists initially showed promising effects on positive and negative symptoms in schizophrenic patients (Meltzer et al., 2004; Spooren et al., 2005). Subsequent reports, however, have been disappointing (Griebel, 2012a). The negative outcome of NK_3R antagonists in clinical trials has been attributed to their physico-chemical properties, such as high clearance, low oral availability or poor brain penetration (Griebel, 2012b). Our results now reveal that NK_3R antagonists might be ineffective against a potential nuclear effect of NK_3Rs that may still play an important role in schizophrenia. The involvement of nuclear NK_3Rs in VTA DA neurons is still unknown. Therefore, the development of new NK_3R antagonists that would also block their NLS sequence would provide a critical tool to investigate their role in gene transcription and behavior.

REFERENCES

Adams MM, Fink SE, Shah RA, Janssen WG, Hayashi S, Milner TA, McEwen BS, Morrison JH (2002) Estrogen and aging affect the subcellular distribution of estrogen receptor-alpha in the hippocampus of female rats. J Neurosci 22:3608–3614.

Calzavara MB, Levin R, Medrano WA, Almeida V, Sampaio AP, Barone LC, Frussa-Filho R, Abilio VC (2011) Effects of antipsychotics and amphetamine on social behaviors in spontaneously hypertensive rats. Behav Brain Res 225:15–22.

Carr DB, Sesack SR (2000) Projections from the rat prefrontal cortex to the ventral tegmental area: target specificity in the synaptic associations with mesoaccumbens and mesocortical neurons. J Neurosci 20:3864–3873.

Cellier E, Barbot L, Regoli D, Couture R (1997) Cardiovascular and behavioural effects of intracerebroventricularly administered tachykinin NK3 receptor antagonists in the conscious rat. Br J Pharmacol 122:643–654.

Chahine MN, Pierce GN (2009) Therapeutic targeting of nuclear protein import in pathological cell conditions. Pharmacol Rev 61:358–372.

Chan J, Aoki C, Pickel VM (1990) Optimization of differential immunogold-silver and peroxidase labeling with maintenance of ultrastructure in brain sections before plastic embedding. J Neurosci Methods 33:113–127.

Chan-Palay V, Jonsson G, Palay SL (1978) Serotonin and substance P coexist in neurons of the rat's central nervous system. Proc Natl Acad Sci U S A 75:1582–1586.

Chen LW, Guan ZL, Ding YQ (1998) Mesencephalic dopaminergic neurons expressing neuromedin K receptor (NK3): a double immunocytochemical study in the rat. Brain Res 780:150–154.

De Brito Gariepy H, Couture R (Blockade of tachykinin NK3 receptor reverses hypertension through a dopaminergic mechanism in the ventral tegmental area of spontaneously hypertensive rats. Br J Pharmacol 161:1868–1884.2010).

Deschamps K, Couture R (2005) The ventral tegmental area as a putative target for tachykinins in cardiovascular regulation. Br J Pharmacol 145:712–727.

Fields HL, Hjelmstad GO, Margolis EB, Nicola SM (2007) Ventral tegmental area neurons in learned appetitive behavior and positive reinforcement. Annu Rev Neurosci 30:289–316.

Flynn FW, Jensen DD, Thakar A, Xu X, Flynn SW, Zhang Z (2011) Neurokinin 3 receptor forms a complex with acetylated histone H3 and H4 in hypothalamic neurons following hyperosmotic challenge. Am J Physiol Regul Integr Comp Physiol 301:R822–831.

Grady EF, Baluk P, Bohm S, Gamp PD, Wong H, Payan DG, Ansel J, Portbury AL, Furness JB, McDonald DM, Bunnett NW (1996) Characterization of antisera specific to NK1, NK2, and NK3 neurokinin receptors and their utilization to localize receptors in the rat gastrointestinal tract. J Neurosci 16:6975–6986.

Griebel G, Beeske S (2012a) Is there still a future for neurokinin 3 receptor antagonists as potential drugs for the treatment of psychiatric diseases? Pharmacol Ther 133:116–123.

Griebel G, Holsboer F (2012b) Neuropeptide receptor ligands as drugs for psychiatric diseases: the end of the beginning? Nat Rev Drug Discov 11:462–478.

Herve D, Pickel VM, Joh TH, Beaudet A (1987) Serotonin axon terminals in the ventral tegmental area of the rat: fine structure and synaptic input to dopaminergic neurons. Brain Res 435:71–83.

Humpel C, Saria A (1993) Intranigral injection of selective neurokinin-1 and neurokinin-3 but not neurokinin-2 receptor agonists biphasically modulate striatal dopamine metabolism but not striatal preprotachykinin-A mRNA in the rat. Neurosci Lett 157:223–226.

Jensen DD, Sundstrom K, Flynn FW (2010) Expression of the nuclear transport protein importin ss-1 and its association with the neurokinin 3 receptor in the rat hypothalamus following acute hyperosmotic challenge. Neuroscience 170:1020–1027.

Jensen D, Zhang Z, Flynn FW (2008) Trafficking of tachykinin neurokinin 3 receptor to nuclei of neurons in the paraventricular nucleus of the hypothalamus following osmotic challenge. Neuroscience 155:308–316.

Kelly A, Vereker E, Nolan Y, Brady M, Barry C, Loscher CE, Mills KH, Lynch MA (2003) Activation of p38 plays a pivotal role in the inhibitory effect of lipopolysaccharide and interleukin-1 beta on long term potentiation in rat dentate gyrus. J Biol Chem 278:19453–19462.

Lee DK, Lanca AJ, Cheng R, Nguyen T, Ji XD, Gobeil Jr F, Chemtob S, George SR, O'Dowd BF (2004) Agonist-independent nuclear localization of the Apelin, angiotensin AT1, and bradykinin B2 receptors. J Biol Chem 279:7901–7908.

Leranth C, Pickel VM (1989) Electron microscopic pre-embedding double immunostaining methods. In: Tract tracing methods 2, recent progress, vol. 2 (Heimer, L., and Zaborsky, L., eds), pp. 129–172. New York: Plenum.

Lessard A, Pickel VM (2005) Subcellular distribution and plasticity of neurokinin-1 receptors in the rat substantia nigra and ventral tegmental area. Neuroscience 135:1309–1323.

Lessard A, Laurin M, Yamaguchi N, Couture R (2004) Central anti-hypertensive effect of tachykinin NK3 receptor antagonists in rat. Eur J Pharmacol 486:75–83.

Lessard A, Grady EF, Bunnett NW, Pickel VM (2007) Predominant surface distribution of neurokinin-3 receptors in non-dopaminergic dendrites in the rat substantia nigra and ventral tegmental area. Neuroscience 144:1393–1408.

Lessard A, Savard M, Gobeil Jr F, Pierce JP, Pickel VM (2009) The neurokinin-3 (NK3) and the neurokinin-1 (NK1) receptors are differentially targeted to mesocortical and mesolimbic projection neurons and to neuronal nuclei in the rat ventral tegmental area. Synapse 63:484–501.

Levin R, Calzavara MB, Santos CM, Medrano WA, Niigaki ST, Abilio VC (2011) Spontaneously hypertensive rats (SHR) present deficits in prepulse inhibition of startle specifically reverted by clozapine. Prog Neuropsychopharmacol Biol Psychiatry 35:1748–1752.

Lin YZ, Yao SY, Veach RA, Torgerson TR, Hawiger J (1995) Inhibition of nuclear translocation of transcription factor NF-kappa B by a synthetic peptide containing a cell membrane-permeable motif and nuclear localization sequence. J Biol Chem 270:14255–14258.

Lu XY, Ghasemzadeh MB, Kalivas PW (1998) Expression of D1 receptor, D2 receptor, substance P and enkephalin messenger RNAs in the neurons projecting from the nucleus accumbens. Neuroscience 82:767–780.

Luo Y, Hattori A, Munoz J, Qin ZH, Roth GS (1999) Intrastriatal dopamine injection induces apoptosis through oxidation-involved activation of transcription factors AP-1 and NF-kappaB in rats. Mol Pharmacol 56:254–264.

Marco N, Thirion A, Mons G, Bougault I, Le Fur G, Soubrie P, Steinberg R (1998) Activation of dopaminergic and cholinergic neurotransmission by tachykinin NK3 receptor stimulation: an in vivo microdialysis approach in guinea pig. Neuropeptides 32:481–488.

Meltzer HY, Arvanitis L, Bauer D, Rein W (2004) Placebo-controlled evaluation of four novel compounds for the treatment of schizophrenia and schizoaffective disorder. Am J Psychiatry 161:975–984.

Misono K, Lessard A (2012) Apomorphine-evoked redistribution of neurokinin-3 receptors in dopaminergic dendrites and neuronal nuclei of the rat ventral tegmental area. Neuroscience 203:27–38.

Nair-Roberts RG, Chatelain-Badie SD, Benson E, White-Cooper H, Bolam JP, Ungless MA (2008) Stereological estimates of dopaminergic, GABAergic and glutamatergic neurons in the ventral tegmental area, substantia nigra and retrorubral field in the rat. Neuroscience 152:1024–1031.

Nalivaiko E, Michaud JC, Soubrie P, Le Fur G, Feltz P (1997) Tachykinin neurokinin-1 and neurokinin-3 receptor-mediated responses in guinea-pig substantia nigra: an in vitro electrophysiological study. Neuroscience 78:745–757.

Otsuka M, Yoshioka K (1993) Neurotransmitter functions of mammalian tachykinins. Physiol Rev 73:229–308.

Overton P, Elliott PJ, Hagan RM, Clark D (1992) Neurokinin agonists differentially affect A9 and A10 dopamine cells in the rat. Eur J Pharmacol 213:165–166.

Oyamada H, Takatsuji K, Senba E, Mantyh PW, Tohyama M (1999) Postnatal development of NK1, NK2, and NK3 neurokinin receptors expression in the rat retina. Brain Res Dev Brain Res 117:59–70.

Paxinos G, Watson C (2007) The rat brain in stereotaxic coordinates. Toronto: Academic Press.

Peters A, Palay SL, Webster HD (1991) The fine structure of the nervous system. New York: Oxford University Press.

Pickard BW, Hodsman AB, Fraher LJ, Watson PH (2007) Type 1 parathyroid hormone receptor (PTH1R) nuclear trafficking: regulation of PTH1R nuclear-cytoplasmic shuttling by importin-alpha/beta and chromosomal region maintenance 1/exportin 1. Endocrinology 148:2282–2289.

Pickel VM, Joh TH, Field PM, Becker CG, Reis DJ (1975) Cellular localization of tyrosine hydroxylase by immunohistochemistry. J Histochem Cytochem 23:1–12.

Pickel VM, Chan J, Nirenberg MJ (2002) Region-specific targeting of dopamine D2-receptors and somatodendritic vesicular monoamine transporter 2 (VMAT2) within ventral tegmental area subdivisions. Synapse 45:113–124.

Regoli D, Boudon A, Fauchere JL (1994) Receptors and antagonists for substance P and related peptides. Pharmacol Rev 46:551–599.

Seabrook GR, Bowery BJ, Hill RG (1995) Pharmacology of tachykinin receptors on neurones in the ventral tegmental area of rat brain slices. Eur J Pharmacol 273:113–119.

Sesack SR, Aoki C, Pickel VM (1994) Ultrastructural localization of D2 receptor-like immunoreactivity in midbrain dopamine neurons and their striatal targets. J Neurosci 14:88–106.

Seybold VS, Grkovic I, Portbury AL, Ding YQ, Shigemoto R, Mizuno N, Furness JB, Southwell BR (1997) Relationship of NK3 receptor-immunoreactivity to subpopulations of neurons in rat spinal cord. J Comp Neurol 381:439–448.

Shirayama Y, Mitsushio H, Takahashi K, Nishikawa T (2000) Differential effects of haloperidol on phencyclidine-induced reduction in substance P contents in rat brain regions. Synapse 35:292–299.

Sladek CD, Stevens W, Levinson SR, Song Z, Jensen DD, Flynn FW (2011) Characterization of nuclear neurokinin 3 receptor expression in rat brain. Neuroscience 196:35–48.

Spooren W, Riemer C, Meltzer H (2005) Opinion: NK3 receptor antagonists: the next generation of antipsychotics? Nat Rev Drug Discov 4:967–975.

Stoessl AJ, Szczutkowski E, Glenn B, Watson I (1991) Behavioural effects of selective tachykinin agonists in midbrain dopamine regions. Brain Res 565:254–262.

Takeuchi Y, Fukunaga K (2004) Dopamine D2 receptor activates extracellular signal-regulated kinase through the specific region in the third cytoplasmic loop. J Neurochem 89:1498–1507.

Tamiya R, Hanada M, Kawai Y, Inagaki S, Takagi H (1990) Substance P afferents have synaptic contacts with dopaminergic neurons in the ventral tegmental area of the rat. Neurosci Lett 110:11–15.

Tremblay L, Kemel ML, Desban M, Gauchy C, Glowinski J (1992) Distinct presynaptic control of dopamine release in striosomal- and matrix-enriched areas of the rat striatum by selective agonists of NK1, NK2, and NK3 tachykinin receptors. Proc Natl Acad Sci U S A 89:11214–11218.

Yang M, Zhang H, Voyno-Yasenetskaya T, Ye RD (2003) Requirement of Gbetagamma and c-Src in D2 dopamine receptor-mediated nuclear factor-kappaB activation. Mol Pharmacol 64:447–455.

(Accepted 3 May 2013)
(Available online xxxx)